Molecular Psychiatry (2005), 10, 1017–1025

www.nature.com/mp

ORIGINAL RESEARCH ARTICLE

# Alternative transcripts and evidence of imprinting of *GNAL* on 18p11.2

JP Corradi[1], V Ravyn[1], AK Robbins[1], KW Hagan[1], MF Peters[1], R Bostwick[1], RJ Buono[2], WH Berrettini[2] and ST Furlong[1]

[1]*Departments of Target Biology and Lead Discovery, AstraZeneca Pharmaceuticals, Wilmington, DE, USA;* [2]*Department of Psychiatry, University of Pennsylvania School of Medicine, Philadelphia, PA, USA*

**Genetic studies implicating the region of human chromosome 18p11.2 in susceptibility to bipolar disorder and schizophrenia have observed parent-of-origin effects that may be explained by genomic imprinting. We have identified a transcriptional variant of the *GNAL* gene in this region, employing an alternative first exon that is 5′ to the originally identified start site. This alternative *GNAL* transcript encodes a longer functional variant of the stimulatory G-protein alpha subunit, $G_{olf}$. The isoforms of $G_{olf}$ display different expression patterns in the CNS and functionally couple to the dopamine D1 receptor when heterologously expressed in Sf9 cells. In addition, there are CpG islands in the vicinity of both first exons that are differentially methylated, a hallmark of genomic imprinting. These results suggest that *GNAL*, and possibly other genes in the region, is subject to epigenetic regulation and strengthen the case for a susceptibility gene in this region.**
*Molecular Psychiatry* (2005) **10,** 1017–1025. doi:10.1038/sj.mp.4001713; published online 26 July 2005

**Keywords:** G-olf; G-proteins; GPCRs; dopamine D1 receptor; CpG islands

Schizophrenia (SZ) and bipolar affective disorder (BPAD, or manic depressive illness) are major psychiatric disorders, each with a worldwide prevalence of ~1%. Both are most often characterized by post-adolescent onset, lifelong persistence, and significant genetic risk. While twin studies have clearly demonstrated heritability for these disorders, penetrance is incomplete, suggesting an environmental component in their etiology. The primary manifestations of SZ and BPAD are disturbances of cognition and mood, respectively. However, there are often cognitive impairments associated with BPAD, as well as profound changes in affect associated with SZ. In addition to some epidemiologic similarities, familial aggregation of related disorders suggests that there may be some shared susceptibility factors. This potential nosological overlap is supported by evidence from genetic linkage studies, in which several susceptibility loci have been identified as common to both disorders.

One such chromosomal region was initially identified by Berrettini *et al*[1] in an affected sib-pair (ASP) analysis of BPAD pedigrees, 18p11.2. This region was subsequently confirmed in several BPAD linkage studies,[2,3] and provided the maximum LOD score in a study of chromosome 18 in 59 German and Israeli SZ pedigrees.[4] It is worth noting that the study by Schwab *et al* included 24 cases of affective disorders, including two with BPAD. Interestingly, a parent-of-origin effect was observed in all of these studies. Specifically, there was a significant *paternal* transmission bias in the BPAD studies. In contrast, Schwab *et al* found SZ linkage in the 12 families with exclusive *maternal* transmission. Such parent-of-origin effects are strongly suggestive of imprinting, an epigenetic phenomenon in which a gene is preferentially expressed from one parental allele.

Of the known genes in the region of chromosome 18p11.2, *GNAL* emerged early as an attractive candidate gene for association studies. *GNAL* encodes the heterotrimeric G-protein stimulatory alpha subunit, $G_{olf}$. Several reports have identified disturbances in G-protein activity and/or expression in BPAD, as well as an effect of subchronic dosing of lithium on $G_{olf}$.[5,6] In addition, $G_{olf}$ is highly expressed in the nucleus accumbens and dorsal striatum, brain regions that are highly relevant to psychosis and psychostimulant drug action. Interestingly, Schwab *et al* found a positive association of a microsatellite marker in intron 5 of the *GNAL* gene with SZ.[4] However, attempts to identify coding region variants of *GNAL* that associate with BPAD or SZ have failed. Given the preponderance of genetic evidence implicating this locus and the known biology of $G_{olf}$, we revisited this gene to search for other potentially significant variants.

Here we report the identification of an alternative transcript derived from the *GNAL* gene, and demonstrate that it encodes a functional G-protein alpha subunit. The more complete genomic structure of

Correspondence: Dr ST Furlong, PhD, Departments of Target Biology and Lead Discovery, AstraZeneca Pharmaceuticals, Wilmington, DE, USA. E-mail: Stephen.Furlong@astrazeneca.com
Received 12 October 2004; revised 26 January 2005; accepted 21 March 2005; published online 26 July 2005

*GNAL* highlights greater similarity to the related gene, *GNAS*. *GNAS* is an imprinted gene, suggesting yet another parallel between these two genes that could be highly relevant to the genetic data reported for BPAD and SZ. We then provide experimental evidence demonstrating that *GNAL* is also subject to epigenetic modification, suggesting that it is an imprinted gene.

## Materials and methods

*Bioinformatics analysis and isolation of $XLG_{olf}$*

A $G_{olf}$ cDNA sequence (L10665) encompassing the full coding region and some of the 5′ and 3′ untranslated regions (UTRs) served as the query in a search of human expressed sequence tag (EST) databanks using the WU-Blast2 algorithm. All partial-length, high-identity matches were manually inspected. Hits with novel sequence were compared to the known *GNAL* gene structure and the draft human genome sequence. A search of mouse EST data suggested a similar splice form. Prediction of CpG islands in regions of the alternative first exons was accomplished with the programs CpGPlot/CpGReport (from the EMBOSS suite of sequence analysis software) using a window of 400 nt, an observed/expected ratio of CG dinucleotides of at least 0.6, and a minimum G + C content of 0.5. Predicted amino-acid sequences were aligned with the ClustalW program. A first-strand cDNA comprising $XLG_{olf}$ was synthesized from RNA from human striatum obtained from Analytical Biological Services (Wilmington, DE, USA), using the gene-specific primer 5′-CCTCACAAGAGCTCATACTGC-3′ and the Superscript first-strand cDNA synthesis kit (Invitrogen, Carlsbad, CA, USA). A full-length cDNA encoding $XLG_{olf}$ was generated by PCR amplification of this cDNA using the primers 5′-CACCATGG GTCTGTGCTACAGTCTG-3′ and 5′-TCACAAGAGCT CATACTGCTT-3′. The $XLG_{olf}$ cDNA was then directionally cloned into the vector pENTR/D-TOPO (Invitrogen). The cloned PCR product was verified by DNA sequencing. Initial attempts to amplify $XLG_{olf}$ were not successful using the Clontech Advantage 2 PCR kit. A PCR product representing $XLG_{olf}$ was only seen when the conditions were modified to use the Clontech GC melt polymerase and GC melt buffer. The reason for this is probably the high GC content of the alternate exon1 that would need to be resolved in order for the PCR amplification to proceed. Of four $XLG_{olf}$ clones sequenced, two were correct and two had different bases inserted most likely due to the PCR conditions.

*Real-time PCR*

The RNA samples in which $G_{olf}$, $XLG_{olf}$, and $\beta$2-microglobulin levels were determined were obtained from commercial suppliers (Ambion, Austin, TX, USA; Stratagene, La Jolla, CA, USA; BD Biosciences Clontech, Palo Alto, CA, USA). All samples had OD 260/280 of 1.8 or greater, as reported by the supplier. Except for the nucleus accumbens (pool of six individuals) and the spinal cord (pool of 49 individuals), all of the RNA samples were derived from one tissue sample. The donors were different for each tissue. Reverse transcription was performed using reagents purchased from Invitrogen. For each RNA sample, cDNA was prepared in triplicate.

Controls for use in absolute quantitation were generated by PCR using plasmids containing $G_{olf}$ or $XLG_{olf}$ and the following oligonucleotides: 5′-CAGGATCCTCATCTGTTTGACG (used for $G_{olf}$ and $XLG_{olf}$), 5′-GGTACCACCATGGGGTGTTTGGGCGGCA CC (used for $G_{olf}$), CAAGGAGGCGAGGAAAGTGA (used for $XLG_{olf}$). The PCR products were purified using the QIAquick PCR Purification kit (Qiagen, Valencia, CA, USA). The purified control fragments were electrophoresed in ethidium-bromide-containing agarose gels and the concentrations were determined by comparing the intensity of the bands with a curve constructed using the fluorescence of standards with known concentrations.

Taqman one-step PCR mastermix, oligonucleotides, and 5′-6FAM/3′-MGBNFQ Taqman probes were purchased from Applied Biosystems (Foster City, CA, USA). Taqman assays were performed using the Applied Biosystems PRISM 7700 Sequence Detection System. $\beta$2-microglobulin levels were determined using human $\beta$2-Microglobulin endogenous control predeveloped assay reagents (Applied Biosystems catalog number 4333766F). For quantitative real-time PCR, the following oligonucleotides were used in detect $G_{olf}$: 5′-AAAGAGCGCCTGGCTTACAAG; 5′-GT TTGACGATGGTGCTTTTCC, and the following oligonucleotides were used to detect $XLG_{olf}$: 5′-GACGCAC CGGCTCCT; 5′-GATGGTGCTTTTCCCAGACTCA. The sequence of the $G_{olf}$ Taqman probe was 5′-ACCAGCC CCCAGGAG and the sequence of the $XLG_{olf}$ Taqman probe was 5′-CCAGCCCCGAGCAGC.

Each cDNA preparation was run in triplicate Taqman QRT-PCR reactions. $G_{olf}$ and $XLG_{olf}$ levels were calculated by comparing the threshold cycle numbers from Taqman reactions with the cDNA samples to standard curves constructed using known copy numbers of $G_{olf}$ or $XLG_{olf}$ purified PCR products (see above). Relative levels of $\beta$2-microglobulin were determined by comparing the threshold cycle numbers from Taqman reactions with the cDNA samples to standard curves constructed using diluted cDNA prepared from total human brain RNA. The levels of Golf or $XLG_{olf}$ were normalized to an endogenous control ($\beta$2-microglobulin) in order to normalize for possible variation in RNA loading (ie dividing $G_{olf}$ or $XLG_{olf}$ levels by the $\beta$2-microglobulin level normalized the samples).

*Generation of recombinant baculoviruses*

The $XLG_{olf}$ cDNA described above was introduced into the cloning vector pENTR/D-TOPO between *Not*I and *Asc*I sites. Recombinant baculovirus encoding human $XLG_{olf}$ was generated with the BaculoDirected™ expression kit (Invitrogen), according to the manufacturer's protocol. The titer of the third-passage

viral stock was determined by plaque assay and used as the working stock.

*Cell culture and membrane preparation*

Sf9 cells were suspended in SF 900 II medium containing penicillin (50 U/ml) and streptomycin (50 $\mu$g/ml) and cultured at 28°C with rotation (125 rpm). Cells were maintained at a density of $2 \times 10^6$ to $4 \times 10^6$ cells/ml. For infection, Sf9 cells at the density of $2 \times 10^6$ cells/ml were infected with baculovirus ($\approx 10^8$ pfu/ml) encoding human dopamine D1A receptor (obtained from Perkin–Elmer Biosignal, Montreal, Canada), human $G_{olf}$ (Perkin–Elmer Biosignal), or human $XLG_{olf}$ at the appropriate multiplicity of infection (MOI). After infection for 48 h, cells were harvested for membrane preparation. Cells were harvested by centrifugation at 500 *g* at 4°C. The cell pellets were washed twice with Dulbecco's phosphate-buffered saline (DPBS) at pH 7.4 and suspended in ice-cold 10 mM Tris-HCl with 5 mM EDTA (TE) (pH 7.4) containing a protease inhibitor cocktail (Roche Applied Science, Indianapolis, IN, USA) and sonicated. Following centrifugation at 1000 *g*, membranes were collected from the supernatant by centrifugation at 20 000 *g* for 30 min at 4°C. The membrane fraction was stored at −80°C in TE containing 5% glycerol.

*[$^3$H]SCH 23390 saturation-binding assay*

Sf9 membrane (2 $\mu$g per reaction) was incubated with 0.018–14.4 nM [$^3$H]SCH 23390 (Amersham, Piscataway, NJ, USA) in the binding buffer (50 mM Tris-HCl, pH 7.4, 5 mM KCl, 5 mM $MgCl_2$, 5 mM EDTA, 1.5 mM $CaCl_2$) at room temperature for 1 h. Nonspecific binding was determined in the presence of 10 $\mu$M (+)-butaclamol (Sigma-Aldrich) in a total volume of 200 $\mu$l. Bound radioligand was collected on GF/C filters using a 96-well cell harvester. Filters were washed five times with 500 $\mu$l of cold 50 mM Tris-HCl buffer (pH 7.4) and filter-bound radioactivity determined by liquid scintillation.

*SDS-PAGE and immunoblot analysis*

Membranes from Sf9 cells expressing the dopamine receptor D1 (DRD1) alone or DRD1 with $G_{olf}$ variants were solubilized in SDS-sample buffer to a final protein concentration of 1 mg/$\mu$l and heated at 80°C for 5 min. Solubilized proteins were separated using SDS-PAGE and 4–12% gradient polyacrylamide gels. Proteins were transferred to polyvinylidene difluoride (PVDF) membranes and probed with rabbit anti-Golf antibody (K-19) (Santa Cruz Reagents, Santa Cruz, CA, USA) diluted at (1 : 5000) and detected with goat anti-rabbit antibody conjugated with horseradish peroxidase (Pierce, Rockford, IL, USA). Immunoreactive bands were visualized by using SuperSignal® West Dura extended-duration substrate (Pierce), according to the manufacturer's instructions.

*[$^{35}$S]GTP$\gamma$S-binding assay*

Membranes from Sf9 cells expressing the DRD1 alone or DRD1 with $G_{olf}$ variants were resuspended in the reaction buffer (20 mM HEPES, pH 7.4, 100 mM NaCl, 10 mM $MgCl_2$, 1 mM EDTA, 1 mM DTT). Agonist-induced [$^{35}$S]GTP$\gamma$S-binding assay was performed for 90 min at room temperature in 96-well microplates, with a volume of 200 $\mu$l per well, and containing 5 $\mu$g of membranes, agonist at a concentration range of $10^{-11}$–$10^{-3}$ M, 10 $\mu$M GDP, and 400 pM [$^{35}$S]GTP$\gamma$S. Nonspecific binding was determined in the presence of 10 $\mu$M unlabeled GTP$\gamma$S. Radioactivity was measured using a Packard Bioscience Top Count NXT Microplate Scintillation microplate reader.

*Data analysis*

Data from [$^3$H]SCH 23390 saturation-binding experiment were fitted to a one-site model to determine the density of DRD1 ($B_{max}$) and the affinity ($K_d$) for [$^3$H]SCH 23390 using the GraphPad Prism program (GraphPad Software Inc.). For agonist-induced [$^{35}$S]GTP$\gamma$S-binding experiments, the percent increase in response was calculated by dividing the specific binding (total minus nonspecific binding) for stimulated membranes by the specific binding of nonstimulated membranes. The $EC_{50}$ and relative maximum response ($E_{max}$) were derived from analysis of the concentration—response curve using nonlinear least-squares regression fit of the GraphPad Prism program. Statistical significance was assessed by analysis of variance (ANOVA), followed by Tukey *post hoc* test.

*Methylation-specific PCR (MSP)*

Brain tissue samples were obtained from autopsies performed on patients at the Veteran's Affairs Medical Center (VAMC). Patients or their legal representative gave written consent for autopsy use of brain tissue for research purposes. The Institutional Review Board of the participating VAMC hospital approved consents and protocols. Only brain tissue obtained from autopsies performed within 24 h or less after death was used from individuals with no clinical signs of psychosis. The brain was exposed by a retroarucular incision and removal of the superior calvarium. After removal of the dura, 10–20 mls of CSF was removed from the lateral ventricle before the brain was extracted. CSF pH was measured to determine the agonal state and the remaining CSF aliquots frozen at −70°C. The whole fresh brain was removed and placed on crushed ice. The brain was hemisected into two hemispheres, 1/2 brain placed in 10% buffered formalin for neuropathological diagnosis; the other 1/2 brain was separated into cerebral hemisphere, cerebellum, and brainstem, placed on a glass plate covered by aluminum foil and then into a −70°C freezer to firm the tissue for cutting, brainstem—15 min, cerebellum—25 min, cerebral hemisphere—40 min. After the appropriate time interval in the

freezer, the brain regions were removed from the freezer and sectioned (brainstem cut into 0.5-cm coronal sections, cerebellum cut into 1.0-cm sagittal sections, cerebrum cut into 16 quick, standardized coronal sections). Punch samples were removed with a 5.0 mm ID stainless steel circular punch from the prefrontal cortex, caudate nucleus head, nucleus accumbens, amygdala, hippocampus, anterior thalamus, substantia nigra, and cerebellum, and immediately placed into cold cryovials and stored in a −70°C freezer until analysis. DNA was extracted from a portion of each unfixed regional brain punch sample (~100 mg wet weight) using phenol chloroform extraction and ethanol precipitation as per standard protocols. DNA was quantified using spectrophotometry and analyzed for integrity using 0.8% agarose gel electrophoresis and ethidium bromide staining.

Genomic DNA extracted from cell lines, peripheral blood or brain were modified using the CpGenome™ Universal DNA Modification Kit (Chemicon International, Temecula, CA, USA). The protocol used was the same as recommended by the manufacturer, with minor modifications. Briefly, 1 μg of genomic DNA in 100 μl of molecular biology grade water was incubated with 200 μM NaOH at 37°C for 15 min. After the incubation, 500 μl of DNA modification reagent I, pH 5, was added and the DNA was then incubated at 55°C for 20 h. The completion of the chemical modification and DNA cleanup was performed as recommended by the manufacturer. Modified DNA was resuspended in 25 μl of 10 mM Tris/0.1 mM EDTA, pH 7.5, and stored at −20°C. MSP was carried out on the modified DNA using primers designed using Chemicon's Primer Design Software or MethPrimer.[7] MSP reactions were carried out using Amplitaq Gold (Applied Biosystems) and the PT-200 DNA Engine (MJ Research, Rneo, NV, USA), using the following conditions: a 9 min initial denaturation step, followed by 35 cycles of amplification using the following conditions: 95°C for 45 s, 55°C for 45 s, and 72°C for 60 s. The PCR reactions were then subjected to electrophoresis in a 1% agarose/TEA gel containing 0.5 μg/ml ethidium bromide. Bands were visualized using GeneGenius Bioimaging System (Syngene, Frederick, MD, USA). The following oligonucleotide primers (MWG Biotech, High Point, NC, USA) were used: 5′-GAACAACAAAAACCGATACG TC and 5′-GTTCGGTTTAAAGTAGATAAGTCGA to detect $XLG_{olf}$ methylated DNA with an expected product size of 186 bp, 5′-TACCAAACAACAAAAAC CAATACAT and 5′-GTTTGGTTTAAAGTAGATAAG TTGA to detect $XLG_{olf}$ unmethylated DNA with an expected product size of 190 bp, 5′-TAAGAGAGTTA GGCGGTCGC and 5′-CCTAATCTAAAATCCCGATAC GAA to detect $G_{olf}$ methylated DNA with an expected size of 218 bp; and 5′-GTGTAAGAGAGTTAGGTGGTT GTG and 5′-TCCCTAATCTAAAATCCCAATACAA to detect unmethylated $G_{olf}$ DNA with an expected product size of 223 bp. PCR products were cloned and sequenced to verify their identities.

## Results

*Identification of an alternate transcript encoded by the GNAL locus*

The *GNAL* gene encodes the olfactory type G-protein alpha subunit, $G_{olf}$. Previous characterization of the human *GNAL* gene structure identified 12 exons with no splice variants detected.[8] In an attempt to identify novel splice forms of the *GNAL* gene, the published cDNA sequence was compared to databases of ESTs. All partial-length, high-identity matches were inspected for the presence of DNA sequence that could identify alternate splice forms or novel exons. One such variant corresponded to a new *GNAL* transcript with an alternative first exon spliced to the known exon 2 of *GNAL*. This new exon, referred to here as exon 1a, maps to human chromosome 18p11.2, approximately 62 kb telomeric to the published exon 1 (referred to here as exon 1b) of *GNAL* (Figure 1a). A transcript containing this alternative first exon and exons 2–12 of *GNAL* (ie, the entire open reading frame) was subsequently verified by RT-PCR from human striatum.

The identification of an alternative first exon illustrates not only a previously unidentified splice form but also an additional transcriptional start site, and presumably a distinct regulatory promoter region. This gene structure is highly similar to the related gene, *GNAS*, which encodes the G-protein alpha subunit $G_{\alpha s}$. As the protein encoded by the 5′ proximal exon 1 of *GNAS* is longer than the originally identified protein, it was named $XLG_{\alpha s}$ (for eXtra Large[9]). Therefore, the alternative transcript of *GNAL* will be referred to as '$XLG_{olf}$'.

An open reading frame in exon 1a of *GNAL* begins with an ATG within a putative Kozak consensus sequence, has an upstream in-frame stop codon, and is conserved between human and mouse. While the predicted amino-acid sequence of $XLG_{olf}$ shares little similarity with the N-terminal region of $XLG_{\alpha s}$, both alternative first exons share a conserved $\beta\gamma$ subunit-binding domain with the originally described proteins (Figure 1b). This evidence suggested that the $XLG_{olf}$ transcript may encode a functional G-protein alpha subunit.

*CNS expression of $G_{olf}$ and $XLG_{olf}$*

PCR analysis of a panel of cDNA libraries from various human CNS regions suggested that the alternate transcripts might have distinct expression patterns (data not shown). Using a Taqman quantitative PCR assay designed to span the exon 1/2 junction of each transcript, we determined the relative distributions of $G_{olf}$ and $XLG_{olf}$ in selected human CNS regions. In agreement with previous studies of the rat and mouse genes,[10,11] the $G_{olf}$ transcript is prominently expressed in the caudate, putamen, and nucleus accumbens. Lower levels of $G_{olf}$ were also detected in the prefrontal cortex, amygdala, hippocampus and hypothalamus, whereas the transcript was barely detected or not detected at all in the spinal

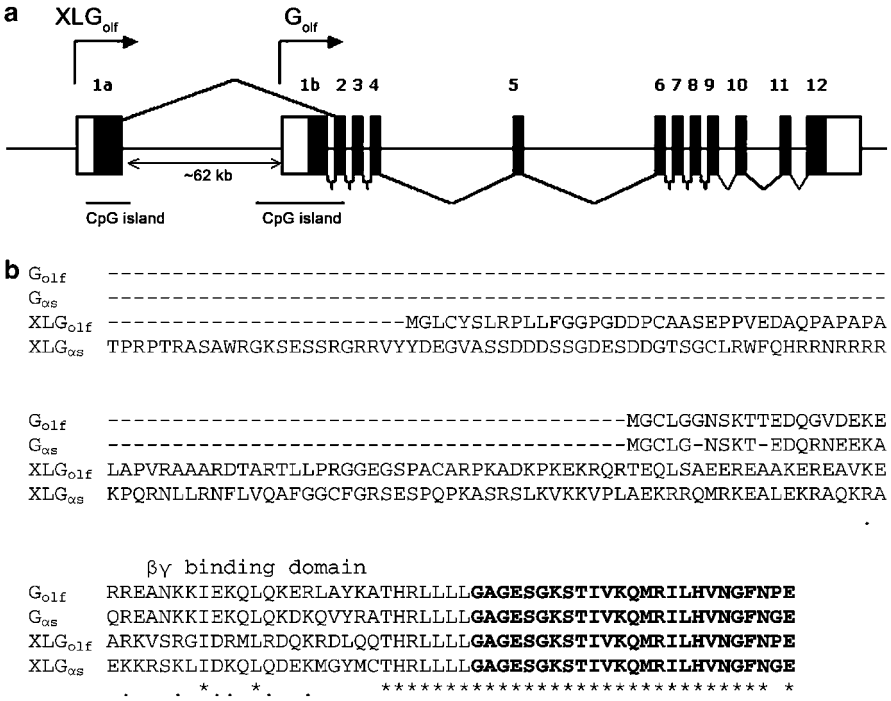


**Figure 1** (a) Schematic of the *GNAL* gene structure. Exons are represented by boxes with the coding region shaded. $XLG_{olf}$ and $G_{olf}$ differ only in their first exons, sharing exons 2–12. The lines underneath represent the positions of the predicted CpG islands using a minimum size of 400 bp (see Materials and methods). (b) An N-terminal amino-acid alignment of the conceptual translations of the long and short transcripts of *GNAL* and *GNAS*. $XLG_{\alpha s}$ contains an additional 240 amino-acids at its N-terminus not shown here. The sequence in bold is that encoded by the common second exons. While the coding region of the original first exons is well conserved, there is little conservation in much of the 'XL' forms. The exception is the region just N-terminal to the exon 2 coding sequence. This region contains the $\beta\gamma$-binding domain of the alpha subunits. Asterisks denote identity, and dots denote similarity.

cord, substantia nigra, and liver (Figure 2). The relative distribution of $XLG_{olf}$ differs markedly from $G_{olf}$, with the most prominent expression in hypothalamus, prefrontal cortex, and the ventral striatum. In those regions where both transcripts were clearly detected, the absolute levels of $XLG_{olf}$ exceeded $G_{olf}$ only in the hypothalamus, substantia nigra, and spinal cord.

*$XLG_{olf}$ encodes a functional G-protein alpha subunit*

While it has been demonstrated that $G_{olf}$ couples with the DRD1,[12,13] interaction of DRD1 with the $G_{olf}$ variant $XLG_{olf}$ is uncharacterized. To evaluate coupling of $G_{olf}$ variants to the DRD1, we introduced these constructs into Sf9 cells and determined agonist-induced [$^{35}$S]GTP$\gamma$s binding, a measure of G-protein activation.

When expressed in Sf9 cells, the apparent molecular weights of $G_{olf}$ and $XLG_{olf}$ were $\approx$44 and $\approx$51 kDa, consistent with molecular weights predicted from their amino-acid sequences (Figure 3a). The molecular weight for $XLG_{olf}$ expressed in HEK 293E cells was comparable (data not shown). Figure 3b shows the saturation binding of [$^3$H]SCH 23390 to DRD1 in Sf9 cells expressing DRD1 alone or DRD1 with $G_{olf}$ or $XLG_{olf}$. The receptor density ($B_{max}$) of Sf9 cells expressing DRD1 alone ($21.3 \pm 0.7$ pmol/mg) was slightly higher than that of Sf9 cells infected with DRD1 plus $G_{olf}$ or DRD1 plus $XLG_{olf}$ ($16.4 \pm 0.6$ and $17.0 \pm 0.8$ pmol/mg, respectively). However, the affinity ($K_d$) of [$^3$H]SCH 23390 to DRD1 in these three cell lines was not substantially different ($0.89 \pm 0.07$ for DRD1 alone, $0.91 \pm 0.13$ for DRD1 plus $G_{olf}$, and $1.01 \pm 0.18$ nM for DRD1 plus $XLG_{olf}$).

Dopamine-activated [$^{35}$S]GTP$\gamma$S binding in Sf9 cells expressing the DRD1 was concentration dependent (Figure 3c). The $EC_{50}$ for dopamine stimulation of DRD1 in Sf9 cells expressing endogenous $G_{\alpha s}$-like G protein, $G_{olf}$, or $XLG_{olf}$ were 84 nM (95% confidence interval (CI), 36.6–192.8 nM), 214 nM (95% CI, 42.3–1083.9 nM), and 179 nM (95% CI, 120.8–266.7 nM), respectively, and did not differ significantly ($P > 0.05$). The efficacy of dopamine for DRD1 in these coinfection experiments was, however, significantly different ($P < 0.0001$). The efficacies of dopamine for DRD1 in Sf9 cells expressing endogenous $G_{\alpha s}$-like G proteins, $G_{olf}$, and $XLG_{olf}$ were $141 \pm 2$, $231 \pm 4$, and $404 \pm 13$%, respectively. These results of dopamine-induced [$^{35}$S]GTP$\gamma$S binding demonstrate that $XLG_{olf}$ functionally coupled to DRD1.

*Differential methylation of GNAL CpG islands*

The genetic linkage of chromosome 18p11.2 to BPAD in multiple studies is associated with a parent-of-origin effect, suggesting genomic imprinting as a mechanism. As the gene structure of *GNAL* displays

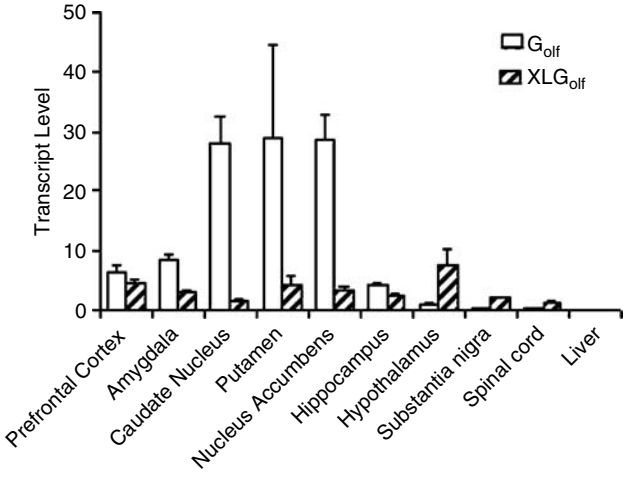


**Figure 2** Quantitation of $G_{olf}$ and $XLG_{olf}$ transcript levels in human CNS tissues and liver using real-time PCR. The results are presented as the absolute amount of $G_{olf}$ or $XLG_{olf}$ transcript in each tissue divided by the relative level of $\beta$2-microglobulin for that tissue (see Materials and methods). The data represent the average of three cDNA preparations from each RNA sample, with each cDNA subjected to Taqman PCR in triplicate; the error bars represent the standard deviation. While in most regions of coexpression $G_{olf}$ is more abundant, $XLG_{olf}$ is the predominant transcript detected in hypothalamus, substantia nigra, and spinal cord.

extensive similarity to that of *GNAS*, a complex imprinted locus,[14] we sought to determine whether the *GNAL* locus is also imprinted. Genomic imprinting involves allele-specific methylation of CpG island regions, defined here as a sequence of at least 400 bp in length with a G + C content of at least 50% and an observed:expected ratio of CG dinucleotides greater than 0.6. An inspection of the 190 kb *GNAL* locus reveals that there are CpG islands in the region of both exon 1a and exon 1b (Figure 1a).

We employed MSP[15] to assess the methylation status of both CpG island regions in the *GNAL* locus. While there have been no reports of methylation of *GNAL* in normal tissue, Costello *et al* reported aberrant and complete methylation of the $G_{olf}$ CpG island in glioma cells.[16] The methylation-sensitive *Not*I restriction site in this region was used to guide the MSP studies, and the T98G glioma cell line served as a positive control for methylated DNA. As expected, only methylated DNA was detected in the T98G cell line by MSP (Figure 4). However, both methylated and unmethylated DNA were detected in genomic DNA from human frontal cortex, substantia nigra (Figure 4), and peripheral blood lymphocytes (not shown), suggesting that *GNAL* is imprinted. Subsequent cloning and DNA sequence analysis of the methylated PCR product showed that all CpG residues within this genomic region amplified were methylated. Differential methylation of the $XLG_{olf}$ CpG island was detected in the T98G cells, frontal cortex, hippocampus, substantia nigra (Figure 4), and peripheral blood (not shown). Although failure to

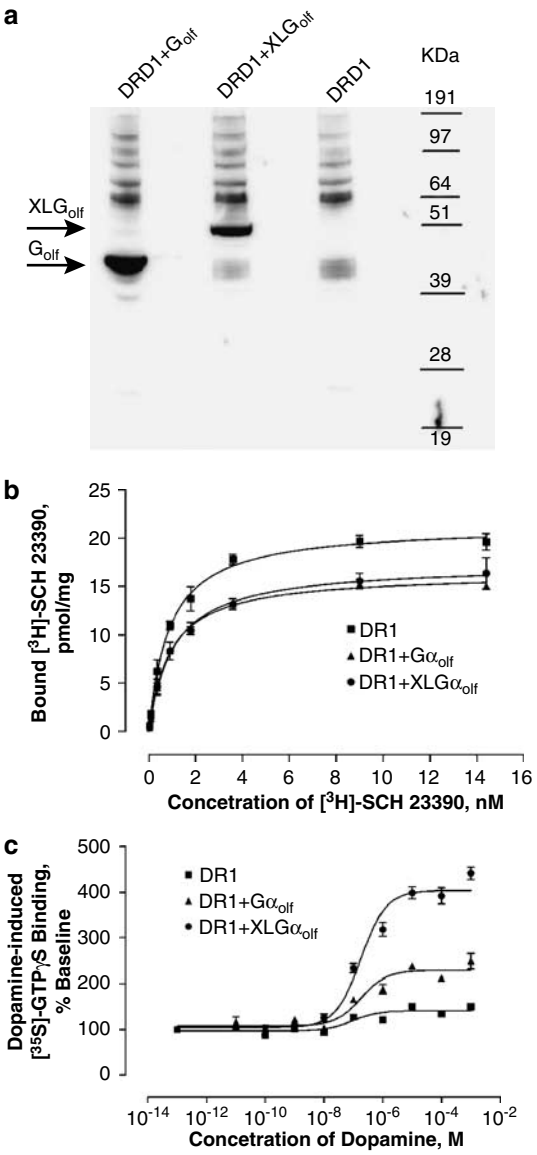


**Figure 3** (a) Expression of $G_{olf}$ and $XLG_{olf}$ in Sf9 cells. Sf9 cells were infected for 48 h with Baculovirus expressing the D1 dopamine receptor alone (MOI = 1) or with $G_{olf}$ (MOI = 5) or $XLG_{olf}$ (MOI = 3) in combination. Lane 1, cells infected with DRD1 and $G_{olf}$; lane 2, cells infected with DRD1 and $XLG_{olf}$; lane 3, cells infected with DRD1 only. (b) Saturation binding of [$^3$H]SCH 23390 to membranes from Sf9 cells infected with DRD1 with or without infection of $G_{olf}$ variants. Membranes from Sf9 cells infected for 48 h with D1 dopamine receptor alone (square) or plus $G_{olf}$ (triangle) or plus $XLG_{olf}$ (circle) at MOI as indicated in (a) were evaluated for saturation binding as described in Materials and methods. Each datum represents the mean ± SE of three experiments performed in triplicate. (c) Dopamine-induced [$^{35}$S]GTP$\gamma$S binding in Sf9 cells expressing DRD1 with or without $G_{olf}$ variants. Membranes from Sf9 cells infected for 48 h with D1 dopamine receptor alone (square) or plus $G_{olf}$ (triangle) or plus $XLG_{olf}$ (circle) (MOI = 1, 5 or 3, respectively) were determined for [$^{35}$S]GTP$\gamma$S binding as described in Materials and methods. Each datum represents the mean ± SE of three experiments performed in triplicate.

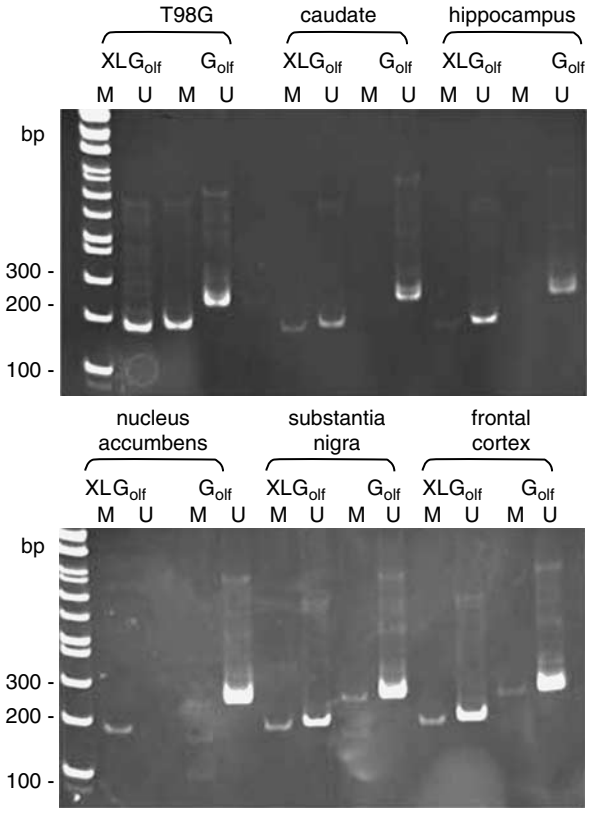


**Figure 4** Detection of methylation in the CpG island regions of $G_{olf}$ and $XLG_{olf}$. MSP was used to detect methylated (M) and unmethylated (U) DNA from the various brain regions indicated, as well as the glioma cell line T98G. See Materials and methods for oligonucleotide primer sequences and expected product sizes. PCR products were cloned and sequenced for verification. Detection of both methylated and unmethylated DNA in each region provides evidence of genomic imprinting at the *GNAL* locus.

detect the methylated or unmethylated state by this method is not definitive, detection of methylation is convincing evidence of epigenetic regulation of a locus. The $G_{olf}$ and $XLG_{olf}$ CpG islands may be methylated in a tissue-specific manner, a phenomenon observed for some other imprinted genes, most notably *GNAS*.

## Discussion

We have identified a longer functional variant of $G_{olf}$ that we have called $XLG_{olf}$. This variant is derived from a large region of the *GNAL* gene that was previously uncharacterized, and is the product of a different transcriptional start site and first exon. Splice variants at the 5′ and 3′ UTRs of the rat *GNAL* gene were identified, but the alternative first exon reported here was not among those findings.[10] However, the availability of the mouse and rat genomes and EST data indicates that the gene structure of *GNAL* is conserved in rodent. The discovery of exon 1a of *GNAL* further extends its degree of similarity to the *GNAS* gene. In addition, we have provided evidence suggesting that *GNAL*, like *GNAS*, is subject to genomic imprinting. To our knowledge, this is the first demonstration of an imprinted locus on human chromosome 18p.

Additional matches to ESTs suggest that there may be at least one other exon 3′ to exon 1a (not shown); however, we were only able to isolate the full-length cDNA reported here. Despite the very similar gene structures of *GNAL* and *GNAS*, the nucleotide sequences of the 5′ ends of the genes do not share a great degree of identity. One clear difference is that there does not seem to be a transcript analogous to the chromogranin-like NESP55[17,18] in the *GNAL* locus.

Since the functional activity of $G_{olf}$ has been previously demonstrated by heterologous coexpression with DRD1 in Sf9 cells,[19] the same system was chosen in this study to evaluate the functional competency of $XLG_{olf}$. Activation of $XLG_{olf}$ through DRD1 was demonstrated by a concentration-dependent dopamine stimulation of [$^{35}$S]GTP$\gamma$S binding. An increase in [$^{35}$S]GTP$\gamma$S binding is a measure of GDP–GTP exchange on the $G_{\alpha}$ subunit as a consequence of receptor-mediated activation. This effect was also seen in cells expressing DRD1 alone, indicating coupling of the receptor to endogenous $G_{\alpha s}$-like protein,[20,21] and in cells coexpressing DRD1 and $G_{olf}$. Although the potency of dopamine is equivalent in all the three cell types, its relative efficacy ($E_{max}$) differs. Cells expressing $XLG_{olf}$ exhibited greater $E_{max}$ than cells expressing $G_{olf}$, which in turn showed greater $E_{max}$ than cells expressing endogenous G$\alpha$s-like protein. Although total receptor number was equivalent in cells expressing either $G_{olf}$ or $XLG_{olf}$ as reflected by $B_{max}$ of [$^{3}$H]SCH23390 binding, an increased $E_{max}$ may reflect a higher ratio of Gprotein to DRD1. However, Western blot analysis showed that $G_{olf}$ expression was greater than $XLG_{olf}$ expression in the cells used for this study. Nevertheless, increases in agonist efficacy may be due to more efficient coupling of G-protein isoforms to receptor. Alternatively, these $G_{olf}$ variants may exhibit differences in GDP–GTP exchange rates.

Both the $G_{olf}$ and $XLG_{olf}$ transcripts are expressed in regions that are relevant to mood and psychosis, such as the nucleus accumbens and prefrontal cortex. In addition, $G_{olf}$ couples to G-protein-coupled receptors (GPCRs), namely the D1 and A2a receptors, that mediate dopaminergic transmission and psychostimulant drug actions in those regions.[22–24] Apparent functional differences between the isoforms would suggest that changes in the relative expression levels of $G_{olf}$ and $XLG_{olf}$ might alter the pharmacology of the GPCRs that couple to them. The quantitative assay we have established will enable the measurement of absolute expression levels of $G_{olf}$ and $XLG_{olf}$ in cells or tissues under different conditions, such as normal and disease states.

Given the multiple independent observations of parent-of-origin effects in linkage studies of SZ and

BPAD with chromosome 18p11.2, the evidence for imprinting at this locus is compelling. It may seem perplexing that studies of different diseases yielding both maternal and paternal parent-of-origin effects could originate from the same locus. However, the example of *GNAS* once again serves to illustrate how such a range of phenotypes and a single imprinted gene can explain opposing transmission biases. *GNAS* encodes distinct transcripts that are either biallelically expressed, maternally imprinted, or paternally imprinted in a tissue-specific manner (for review, see Weinstein *et al*[25]). We have not determined the specific allele that is imprinted for each of the *GNAL* transcripts, as this requires identification of a polymorphism in the transcribed region, access to DNA and RNA from an individual, and unambiguous parental genotypes. However, re-sequencing of *GNAL* CpG island regions is likely to provide some polymorphic markers that would allow for such a determination.

DNA methylation that constitutes the 'imprint' most often results in repression of transcription. While it is difficult to provide evidence of allele-specific expression in human tissue for the reasons stated above, Costello *et al*[16] did correlate hypermethylation of the $G_{olf}$ CpG island region with reduced expression in glioma cells. This suggests that methylation of one parental allele would result in silencing, or partial silencing, of *GNAL* transcription.

Imprinted genes are often found in clusters in the genome, with an imprinting control region mediating allele-specific expression of multiple genes.[26] *GNAL* is located in a gene-rich region containing both interesting biological candidates for susceptibility and genes that have been positively associated with psychosis. MPPE1, a brain-specific metallophosphoesterase, is transcribed in the opposite orientation as *GNAL*, and the two genes have overlapping 3′ UTRs.[27] IMPA2, located within 100 kb of *GNAL*, is an inositol phosphatase that has been reported to be associated with both SZ[28] and more recently BPAD.[29] It is possible that these or other genes in the region of *GNAL* may also be subject to epigenetic regulation.

*GNAL* itself has been investigated as a candidate gene for both BPAD and SZ for several years. To date, no coding region variants of $G_{olf}$ have been reported. A strong association with SZ was reported for a microsatellite in the fifth intron,[4] whereas other genetic studies of BPAD and unipolar depression using intronic *GNAL* polymorphisms have yielded negative results.[30–32] The results presented here identify a new region of the *GNAL* gene that has escaped investigation in previous studies. Nevertheless, many validated SNPs have been identified in this region and are available in public databases (see RefSeq NM_182978). Further genetic analysis is warranted.

## Acknowledgements

We gratefully acknowledge Greg Golden at the Veterans Affairs Medical Center in Coatesville, PA, for providing the human brain tissue.

## References

1 Berrettini WH, Ferraro TN, Goldin LR, Weeks DE, Detera-Wadleigh S, Nurnberger Jr JI *et al.* Chromosome 18 DNA markers and manic-depressive illness: evidence for a susceptibility gene. *Proc Natl Acad Sci USA* 1994; **91**: 5918–5921.
2 Stine OC, Xu J, Koskela R, McMahon FJ, Gschwend M, Friddle C *et al.* Evidence for linkage of bipolar disorder to chromosome 18 with a parent-of-origin effect. *Am J Hum Genet* 1995; **57**: 1384–1394.
3 Nothen MM, Cichon S, Rohleder H, Hemmer S, Franzek E, Fritze J *et al.* Evaluation of linkage of bipolar affective disorder to chromosome 18 in a sample of 57 German families. *Mol Psychiatry* 1999; **4**: 76–84.
4 Schwab SG, Hallmayer J, Lerer B, Albus M, Borrmann M, Honig S *et al.* Support for a chromosome 18p locus conferring susceptibility to functional psychoses in families with schizophrenia, by association and linkage analysis. *Am J Hum Genet* 1998; **63**: 1139–1152.
5 Manji HK, Lenox RH. The nature of bipolar disorder. *J Clin Psychiatry* 2000; **61**(Suppl 13): 42–57.
6 Miki M, Hamamura T, Ujike H, Lee Y, Habara T, Kodama M *et al.* Effects of subchronic lithium chloride treatment on G-protein subunits (Golf, Ggamma7) and adenylyl cyclase expressed specifically in the rat striatum. *Eur J Pharmacol* 2001; **428**: 303–309.
7 Li LC, Dahiya R. MethPrimer: designing primers for methylation PCRs. *Bioinformatics* 2002; **18**: 1427–1431.
8 Vuoristo JT, Berrettini WH, Overhauser J, Prockop DJ, Ferraro TN, Ala-Kokko L. Sequence and genomic organization of the human G-protein Golfalpha gene (*GNAL*) on chromosome 18p11, a susceptibility region for bipolar disorder and schizophrenia. *Mol Psychiatry* 2000; **5**: 495–501.
9 Kehlenbach RH, Matthey J, Huttner WB. XL alphas is a new type of G protein. *Nature* 1994; **372**: 804–809.
10 Herve D, Rogard M, Levi-Strauss M. Molecular analysis of the multiple Golf alpha subunit mRNAs in the rat brain. *Brain Res Mol Brain Res* 1995; **32**: 125–134.
11 Belluscio L, Gold GH, Nemes A, Axel R. Mice deficient in G(olf) are anosmic. *Neuron* 1998; **20**: 69–81.
12 Zhuang X, Belluscio L, Hen R. G(olf) alpha mediates dopamine D1 receptor signaling. *J Neurosci* 2000; **20**: RC91.
13 Corvol JC, Studler JM, Schonn JS, Girault JA, Herve D. Galpha(olf) is necessary for coupling D1 and A2a receptors to adenylyl cyclase in the striatum. *J Neurochem* 2001; **76**: 1585–1588.
14 Hayward BE, Moran V, Strain L, Bonthron DT. Bidirectional imprinting of a single gene: *GNAS*1 encodes maternally, paternally, and biallelically derived proteins. *Proc Natl Acad Sci USA* 1998; **95**: 15475–15480.
15 Herman JG, Graff JR, Myohanen S, Nelkin BD, Baylin SB. Methylation-specific PCR: a novel PCR assay for methylation status of CpG islands. *Proc Natl Acad Sci USA* 1996; **93**: 9821–9826.
16 Costello JF, Fruhwald MC, Smiraglia DJ, Rush LJ, Robertson GP, Gao X *et al.* Aberrant CpG-island methylation has non-random and tumour-type-specific patterns. *Nat Genet* 2000; **24**: 132–138.
17 Ischia R, Lovisetti-Scamihorn P, Hogue-Angeletti R, Wolkersdorfer M, Winkler H, Fischer-Colbrie R. Molecular cloning and characterization of NESP55, a novel chromogranin-like precursor of a peptide with 5-HT1B receptor antagonist activity. *J Biol Chem* 1997; **272**: 11657–11662.
18 Weiss U, Ischia R, Eder S, Lovisetti-Scamihorn P, Bauer R, Fischer-Colbrie R. Neuroendocrine secretory protein 55 (NESP55): alternative splicing onto transcripts of the *GNAS* gene and posttranslational processing of a maternally expressed protein. *Neuroendocrinology* 2000; **71**: 177–186.
19 Gille A, Seifert R. Co-expression of the beta2-adrenoceptor and dopamine D1-receptor with Gsalpha proteins in Sf9 insect cells: limitations in comparison with fusion proteins. *Biochim Biophys Acta* 2003; **1613**: 101–114.
20 George SR, Lee SP, Varghese G, Zeman PR, Seeman P, Ng GY *et al.* A transmembrane domain-derived peptide inhibits D1 dopamine receptor function without affecting receptor oligomerization. *J Biol Chem* 1998; **273**: 30244–30248.
21 Leopoldt D, Harteneck C, Nurnberg B. G proteins endogenously expressed in Sf 9 cells: interactions with mammalian histamine

receptors. *Naunyn-Schmiedeberg's Arch Pharmacol* 1997; **356**: 216–224.
22 Herve D, Le Moine C, Corvol JC, Belluscio L, Ledent C, Fienberg AA *et al.* Galpha(olf) levels are regulated by receptor usage and control dopamine and adenosine action in the striatum. *J Neurosci* 2001; **21**: 4390–4399.
23 Zahniser NR, Simosky JK, Mayfield RD, Negri CA, Hanania T, Larson GA *et al.* Functional uncoupling of adenosine A(2A) receptors and reduced response to caffeine in mice lacking dopamine D2 receptors. *J Neurosci* 2000; **20**: 5949–5957.
24 Zhang D, Zhang L, Lou DW, Nakabeppu Y, Zhang J, Xu M. The dopamine D1 receptor is a critical mediator for cocaine-induced gene expression. *J Neurochem* 2002; **82**: 1453–1464.
25 Weinstein LS, Yu S, Warner DR, Liu J. Endocrine manifestations of stimulatory G protein alpha-subunit mutations and the role of genomic imprinting. *Endocr Rev* 2001; **22**: 675–705.
26 Reik W, Walter J. Genomic imprinting: parental influence on the genome. *Nat Rev Genet* 2001; **2**: 21–32.
27 Vuoristo JT, Ala-Kokko L. cDNA cloning, genomic organization and expression of the novel human metallophosphoesterase gene MPPE1 on chromosome 18p11.2. *Cytogenet Cell Genet* 2001; **95**: 60–63.
28 Yoshikawa T, Kikuchi M, Saito K, Watanabe A, Yamada K, Shibuya H *et al.* Evidence for association of the myo-inositol monophosphatase 2 (IMPA2) gene with schizophrenia in Japanese samples. *Mol Psychiatry* 2001; **6**: 202–210.
29 Sjoholt G, Ebstein RP, Lie RT, Berle J, Mallet J, Deleuze JF *et al.* Examination of IMPA1 and IMPA2 genes in maniac-depressive patients: association between IMPA2 promoter polymorphisms and bipolar disorder. *Mol Psychiatry* 2003; **23**: 23.
30 Berrettini WH, Vuoristo J, Ferraro TN, Buono RJ, Wildenauer D, Ala-Kokko L. Human G(olf) gene polymorphisms and vulnerability to bipolar disorder. *Psychiatr Genet* 1998; **8**: 235–238.
31 Tsiouris SJ, Breschel TS, Xu J, McInnis MG, McMahon FJ. Linkage disequilibrium analysis of G-olf alpha (*GNAL*) in bipolar affective disorder. *Am J Med Genet* 1996; **67**: 491–494.
32 Zill P, Engel R, Baghai TC, Zwanzger P, Schule C, Minov C *et al.* Analysis of polymorphisms in the olfactory G-protein Golf in major depression. *Psychiatr Genet* 2002; **12**: 17–22.